A Novel-Fed Fixed Frequency-Source Dielectric Resonator for Frequency Stability-Dependent Applications

Seyi Stephen Olokede[1], Babu Sena Paul[1], Mohd Fadzil Ain[2]

[1]Department of Electrical & Electronic Engineering Technology,
University of Johannesburg, 2028 Doornfontein, Johannesburg, South Africa
[2]School of Electrical & Electronic Engineering,
University of Science Malaysia, 14300 Nibong Tebal, Penang, Malaysia.

Abstract- A simple and novel microstrip-fed dielectric resonator (DR) as fixed frequency source is proposed design. The feed mechanism consists of three microstrip line sections, each of a width approximately equal to its characteristic impedance. The DR located at the centre of the grounded laminate Roger RO4003C Duroid microwave board of size 18 × 18 sq. mm, with a substrate height of 0.813 mm, dielectric constant $\varepsilon_r = 3.38 \pm 0.05$, and a metallization of 35μm is excited by these microstrip lines such that port 1 and 2 are oppositely edges-coupled to the DR in a balanced parallel arrangement, whereas, the third microstrip line is orthogonal to the microstrip feed line excited by port 2. Each of the feed line are located at a coupling space (β) of 0.24 mm away from the DR, whereas, the third orthogonal microstrip line is capacitively coupled through the excitation of port 1 and 2. Both the measured and numerical results agreed reasonably.

1. INTRODUCTION

It is not uncommon in recent times to see systems relying massively on high quality time and frequency sources. In most cases, a drift of frequency could lead to grave consequences that in a way could influence the quality of the carrier signal, degrade system efficiency, and as such affects the stability control performance, as its applicable in tracking, missiles, guidance, navigations, communications, and radar applications to mention but a few. Consequently, frequency instability characterization (and sources) has become of great concern to many engineers working in various fields. The predominant frequency-determining element in an oscillator is its resonator, which acts as a frequency discriminator. Different alternative frequency stability sources have been reported in literatures, too many to be concisely cited. For instance, Tsironis [1] proposed design an idea of DRO temperature stability modeling. Such approach results in a model that furnishes limits and concepts for oscillation power, fixed frequency source, and pre-requisites' for an optimal resonator constituents. Also, investigations of the fixed frequency source with respect to temperature of a GaAs FET dielectric resonator oscillator (DRO), and the two ports excited DR as a band rejection filter were reported in many literatures, whereas, Jinyong *et al* reported microwave DRO long term fixed frequency source with regards to the effect of environmental and internal degradation processes [2]-[5]. In all of these, emphasis were placed on the relationship between temperature and the fixed frequency source, or focuses more on the long term degradation procedure and fixed frequency source of the DRO, saves in few literatures, where environmental and internal degradation were examined [6].

In this paper, a triple microstrip sections feed mechanism capitalizing on the dynamics of voltage allocation on transmission line is proposed design. The resonator is made of CCTO ($CaCuTi_4O_{12}$) cylindrical DR with a loss tangent (tan δ) equal to 0.028, and an aspect ratio of less than 0.45. Subsequently, we firstly intend to establish the principle behind the third orthogonal microstrip line section, and to what extent does it affects frequency instability even using the popularly reported temperature stable DR, with respect to 1) the effect of the section length, 2) the coupling coefficient (k), and, 3) the Q factor. Though it has been established that DR inherently exhibits very little fluctuations upon excitation, thereby producing a more stable frequency resonance with attendant improvement in phase noise. As such, the proposed design becomes attractive and offer to be a good candidate for stable resonance source. The obvious reason of its attractiveness is as a result of the nether frequency restriction foisted by the eventual expanse size of the resonator. Though the reduced Q-factor of small resonators imposes a restriction on the upper frequency band, the dimensions of the small resonator also become too unappreciable to efficiently be energized with the microstrip feed line. The fixed frequency source and the degree of its control therefore relies substantially on the excitation between the gate transmissions line of the DRO and the DR, seeing the tighter the coupling the greater the tuning range. Parametric studies carried out indicate that both the reflection coefficient ($|S_{11}|$), as well as the insertion loss ($|S_{12}|$) of the proposed design structure are reasonably influenced by 1) the length of the third microstrip section, 2) the location, and finally, 3) its geometry.

2. THE DESIGN THEORY

The voltage allocation over the length of open-ended microstrip line demonstrates the existence of periodic voltage maxima (antinodes) and voltage minima (nodes) from the open-circuited end to the source as demonstrated in Figure 2 of [7]-[8]. This voltage maxima condition and its impedance is periodic at every λ/2 away from the generator. In effect, the optimal radiation will be experienced at the open-circuited end of Figure 1(a) provided that the length of the microstrip line is equal to $n\lambda/2$. Figure 1(b) shows both the *E*- and *H*-fields of Figure 1(a) in *yz*-plane at the instance of the applied voltage which causes current I_1 to flow through the line. Similarly, the fringing field effect at the discontinuity (i.e. the open-circuited end) of the transmission line of Figure 1(a) causes an extension of the line electrical length due to fringing. Though the line is physically terminated at the target length, the fields do not truncate abruptly. Instead, it increase moderately farther as a result of fringing field.

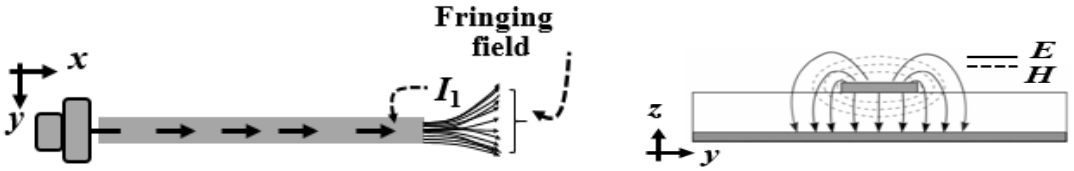

(a) (b)

Figure 1: Current effect on microstrip line. (a) Open-ended line, (b) EM field of open-ended line at *xy*-plane

Figure 2(a) depicts the proposed design feeding mechanism with its operational functionality based on 1) the voltage allocation on the open-circuited microstrip line, and 2) the fringing filed effect at the discontinuity end. The length of the microstrip line (L_1) will experience maximum radiation at every antinode provided the segmented length is equals to $n\lambda/2$. The combination of the fields due to the presence of the antinode as well as the fringing field effect at the open-circuited end causes the electrical length of line L_1 to extend (though physically the same). The extension causes an overlap between line L_1 and line L_3 shown in Figure 2(b), hence causing the current I_1 to flow through the lines when excited by ports 1. Thus, both lines in effect becomes one. Similar scenario happens to the line L_2 with respect to L_3, such that the combinations of these effects leads to the coupling of the DR in such an arrangement constituting a balanced parallel-fed mechanism to ensure stronger coupling. There is therefore an assumption that if the excitation voltages at both ports are constant and equal, and that there is an existence of symmetry about line L_3, then the superposition effect of the current I_T (= $I_1 + I_2$ where I_2 is the current as a result of port 2) may be constant. If this assumption is true, then the three microstrip lines (L_1, L_2, and L_3) becomes L_T (= $L_1 + L_2 + L_3$). The coupling effect may also be constant. For this to be so, it must have been assumed that losses have been mitigated, in particular the radiation losses. Furthermore, a vial may be inserted as shown in Figure 2(b) in order to create a low impedance path to return the current in an arrangement analogous to feedback loop. The effect of this will sustain the constancy of the fields, and also disallow line L_2 from experiencing fringing field. Equation (1) reflects the effect of resonance variation with respect to the microstrip feed length, where L_T is the entire microstrip feed length, *k* is the coupling coefficient, $R = 1$ is the reflection

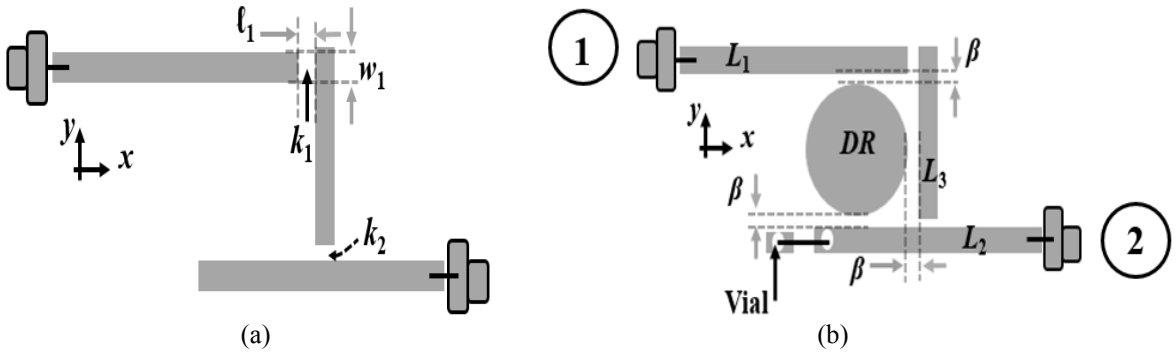

(a) (b)

Figure 2: The proposed design design, (a) The feed arrangement, (b) The geometry.

coefficient of the complex impedance load corresponding to open-end stub, λ is the physical length of the transmission feed line, and *Q* is the Q factor. It is evident by this equation that resonance variation is directly

dependent on the k, and L_T. It is indirectly dependent on Q and λ. It can be established by Equation (1) that the resonance variation (Δf) is equal to zero at every $n\lambda/4$ and non-zero otherwise. To therefore obtain invariant resonance, L_T must equal to $((2n + 1)\lambda)/4$. Any exception will lead to extra equivalent length of $\Delta\ell$ (with an added length of $\Delta\ell + \lambda/4$) due to fringing effect.

$$\Delta f = -\frac{k_n R}{2Q} Sin 4\pi \frac{L_T}{\lambda} \quad (1)$$

Equation (2) defines the coupling space (β) with respect to the coupling coefficient (k). By this equation, resonance variation also depends on β. It is therefore contingent that β must theoretically be zero if resonance variation must be avoided. Unfortunately, this is practically impossible due to etching limitation, in particular when metallic radiator is used. Using DR overcome the challenges of etching limitation, as it can easily be placed at any location. The relation $\Delta f = \beta R/2Q$ if carefully implemented could be used to determine the optimal coupling space.

$$\beta = k_n Sin 4\pi \frac{L_T}{\lambda} \quad (2)$$

3. THE DESIGN

The characteristic impedance of the lines (L_1, L_2, & L_3) is first determined to be approximately equal to 50 Ω with a corresponding width (w) of 1.9 mm using transmission line impedance calculator available in CST microwave studio. The length L_1 is determined to be equal to $n\lambda/2$ (= 16 mm) in order to coincides with maxima positions. Calculation based on λ/2 automatically disobey Equation (1), and by effect creates fringing field effect at the open-circuited end of the line. L_3 position is parametrically obtained using CST such that the coupling space between L_1 and L_3 is saturated with the fields' intensities due to fringing field of L_1. L_3 is so positioned such that the electrical length of L_1 (as a result of fringing field of L1) overlap the physical length of L_3 by an amount equal to the coupling space. The length L_3 is determined to be $n\lambda/2$ (= 8) in the similitude of L_1. To ensure that there exist no fringing effect at the open-circuited end of L_2, the length is determined to be $n\lambda/2 + \lambda/4$ (= 15 mm) where λ is calculated to be 4 mm at the resonance frequency of 10 GHz. A vial is then inserted to ground the fringing field and to establish a feedback loop. Subsequently, a cylindrical DR is used because of its Q factor-resonant frequency relationship which indeed depends on the radius/height ratio. This is done to ensure that the DR's aspect ratio (in particular the ratio of DR thickness to its diameter), is in the neighborhood of 0.35 to 0.45 such that the resonator does not becomes resistive at other frequencies. It is then configured to excite $TE_{01\delta}$ in order to prevent interference of spurious resonant modes, and as such, prevent oscillations at undesired frequencies. The dimensions of the cylindrical DR for $TE_{01\delta}$ mode is determined with the diameter (a) = 5.1 mm, thickness (h) = 2.95 mm, and relative permittivity (ε_r) = 55. The higher the Q factor, the lower is the resonance shift as stated by the relation $\Delta f = (s-1)f_0/Q(s)^{0.5}$ where s is the maximum allowable standing wave ratio (VSWR)[9]-[11]. Therefore, a DR with a high Q of about 10×10^3 is used. Parametric optimization is then done to efficiently position the DR such that it is optimally excited using Δf Equation (reported in Section 2) along with the CST optimization. Since the radiation losses increases with increase of substrate height (h), and relative permittivity (ε_r) according to the relation $(h(\varepsilon_r)^{0.5}/\lambda)$, the resulting design is prototyped on a low permittivity and slim Roger duroid laminate microwave board bearing in mind that a lower effective dielectric constant (ε_{eff}) shifts the resonance frequency and decrease the Q factor . The measurement is done using 45 MHz – 50 GHz E8364A PNA series network analyzer.

4. RESULTS AND DISCUSSIONS

Table 1 summarizes the resonance responses of the proposed design with respect to varying coupling spacing using CST, HFSS, and in measured results. It is evident that frequency variance occurred but moderately. The resonance average at about 10 GHz notwithstanding the fact that resonance variance is dependent on the coupling space. The implication of this is that the proposed design method is suitable for stable resonance source. Figure 1 depicts the stability of resonance based on measured and numerical results using CST and HFSS. Resonance hover around 10 GHz except that of measured result that occurred a little above 10.125 GHz. The discrepancy is due to the inability to accurately position the propose design at the precisely antinodes location during fabrication compare to what is obtainable during simulation. Table 2 explains the obtained insertion loss ($|S_{12}|$ which in itself is a loss quantity) by measurement and numerical results from CST and HFSS.

Table 1: Effect of coupling space on resonance.

Coupling Space (mm)	Resonant Frequency (GHz)		
	CST	HFSS	Measured
0.1	10.060	10.020	10.201
0.3	10.055	10.070	10.200
0.5	10.065	10.010	10.206
0.7	10.045	10.080	10.208
0.9	10.051	10.091	10.203

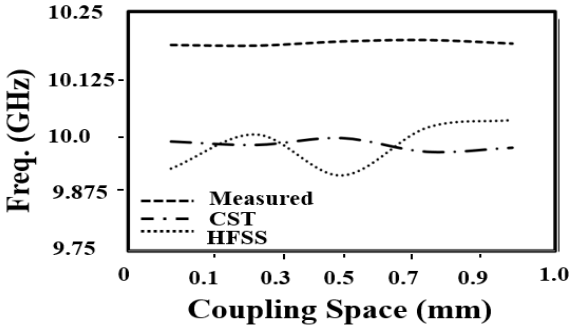

Figure 1: Resonance frequency vs. coupling space.

Table 2: Effect of coupling space on $|S_{12}|$ in dB.

Coupling Space (mm)	Insertion Loss (dB)		
	CST	HFSS	Measured
0.1	-0.200	-0.103	-0.421
0.3	-0.336	-0.170	-0.566
0.5	-0.817	-0.410	-0.909
0.7	-1.092	-0.577	-1.550
0.9	-1.217	-0.585	-1.833

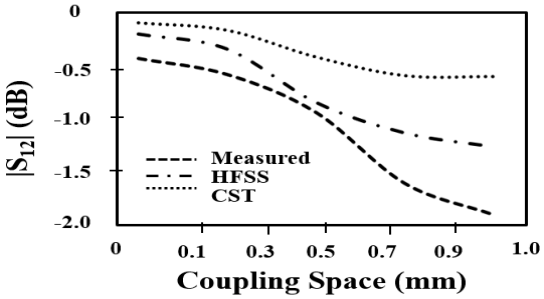

Figure 2: Insertion loss vs. coupling space.

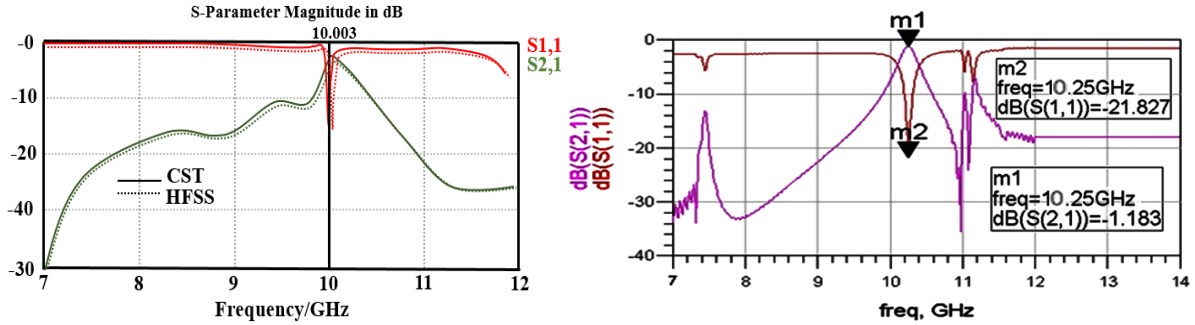

(a) (b)

Figure 3: Optimized S-parameter results of the proposed design. (a) Simulation, (b) Measured

Table 3: Simulated and measured results summary

Parameters	Simulations		Measured
	CST	HFSS	
$\underset{\text{dB}}{\lvert S_{12}\rvert}$	-1.08	-1.02	-1.183
$\underset{\text{dB}}{\lvert S_{11}\rvert}$	-16.10	-16.08	-21.827
$\underset{\text{GHz}}{f_0}$	10.002	10.003	10.250

The $|S_{12}|$ is less than -3 dB across the coupling space. In Figure 2, $|S_{12}|$ bottomed at $\beta = 0.9$ mm to about -2 dB. Both measured and simulated results agreed reasonably till $\beta > 0.5$ mm when the CST and HFSS results diverged. Nonetheless, the measured and CST results agreed moderately. Figure 3 depicts the optimized measured and simulated results of the proposed design, whereas, Tables 3 summarizes the proposed design performance metrics

at 10 GHz target resonance frequency. Comparing the relevant simulated results with the measured indicate a $|S_{12}|$ differential of 9.54% for CST-measured, and 15.98% for HFSS-measured. Similarly, $|S_{11}|$ demonstrates 35.55% for CST-measured, and 35.72% HFSS-measured in favor of the measured result. The reason for these differential has earlier been identified. More importantly, the resonance shift (Δf) is 2.8% for CST-measured, and 2.47% for HFSS-measured. It is evident therefore that resonance shift of about 2.47% is marginal.

5. CONCLUSIONS

A moderately stable frequency source has been demonstrated. The stable frequency source has been investigated using the commercially available numeric solver such as CST microwave studio and ANSY HFSS. The resulting design is fabricated, measured, and these results are compared to determine the degree of agremment. The reason for discrepancy was identifed and reported. On a genaral note, the results agreed reasonably.

REFERENCES

1. Tsironis C., and V. Pauker, “Temperature Stability of GaAs MESFET Oscillators Using Dielectric Resonators”, IEEE Trans. Microwave Theory Tech, Vol. MTT-31, No. 3, 312 – 314, 1983.
2. Abe H., Y. Takayama, A. Higashisaka, and H. Takamizawa, "A Highly Stabilized Low-Noise GaAs FET Integrated Oscillator with a Dielectric Resonator in the C Band, " *IEEE Transactions on Microwave Theory and Techniques,* Vol. 26, No. 3, 156-162, Mar 1978.
3. G. S. Dow, D. Sensiper, and J. M. Schellenberg, "Highly Stable 35 GHz GaAs FET Oscillator," *IEEE MTT-S International Microwave Symposium Digest,* 589-591, 2-4 June 1986.
4. Abe H., Y. Takayama, A. Higashisaka, and H. Takamizawa, "A stabilized, low-noise GaAs FET integrated oscillator with a dielectric resonator at C-band,” *IEEE International Solid-State Circuits Conference. Digest of Technical Papers,* 168-169, 16-18 Feb. 1977
5. Ishihara O., T. Mori, H. Sawano, and M. Nakatani, "A Highly Stabilized GaAs FET Oscillator Using a Dielectric Resonator Feedback Circuit in 9-14 GHz," *IEEE Transactions on Microwave Theory and Techniques,* Vol. 28, no. 8, 817-824, Aug 1980
6. Jinyong Yao; Haibo Su; Xiaogang Li, "Study of microwave Dielectric Resonator Oscillator long term frequency stability," 2010 IEEE International Conference on Wireless Information Technology and Systems, 1-4, Aug. 28 2010-Sept. 3 2010.
7. Olokede S. S., “A Quasi-Lumped Element Series Array Resonator Antenna,” *Radioengineering*, Vol. 24, No. 3, 695-702, September 2015.
8. Ain M. F., Y. M. A. Qasaymeh, Z. A. Ahmad, M. A. Zakariya, M. A. Othman, A. A. Sulaiman, A. Othman, S. D. Hutagalung, and M. Z. Abdullah, "A novel 5.8 GHz high gain array dielectric resonator antenna," *Progress In Electromagnetics Research C*, Vol. 15, 201-210, 2010.
9. Drossos D., Z. Wu and L.E. Davis, “Theoretical and experimental investigation of cylindrical Dielectric Resonator Antennas”, Microwave and Optical Technology Letters, Vol. 13, No. 3, pp. 119-123, October 1996.
10. Petosa A., “Dielectric Resonator Antenna Handbook”, Artech House, Boston/London, 2007
11. Luk K.M, and K.W Leung, “Dielectric Resonator Antennas”, Electronic & Electrical Engineering Research Studies